PNAS USA. In press. 2008

Rapid signal transduction in living cells is a unique feature of mechanotransduction

Sungsoo Na[*], Olivier Collin[*], Farhan Chowdhury[*], Bernard Tay[*], Mingxing Ouyang[†], Yingxiao Wang[†], Ning Wang[*‡]

[*]Department of Mechanical Science and Engineering, [†]Department of Bioengineering, University of Illinois at Urbana-Champaign, Urbana, IL 61801 USA

Key words: mechanical force, growth factor, cytoskeleton, prestress, microtubule

Author contributions

SN and NW designed research; SN, OC, FC, MO performed research; SN and BT analyzed data; NW, SN, and YW wrote the paper.

The authors declare no conflict of interest.

[‡]To whom correspondence should be addressed: nwangrw@uiuc.edu

Abstract

It is widely postulated that mechanotransduction is initiated at the local force-membrane interface by inducing local conformational changes of proteins, similar to soluble ligand-induced signal transduction. However all published reports are limited in timescale to address this fundamental issue. Using a FRET-based cytosolic Src reporter in a living cell, we quantified changes of Src activities as a local stress via activated integrins was applied. The stress induced rapid (<0.3 s) activation of Src at remote cytoplasmic sites, which depends on the cytoskeletal prestress. In contrast, there was no Src activation within 12 s of soluble epidermal growth factor (EGF) stimulation. A 1.8-Pa stress over a focal adhesion activated Src to the same extent as 0.4 ng/ml EGF at long times (minutes), and the energy levels for mechanical stimulation and chemical stimulation were comparable. The effect of both stress and EGF was less than additive. Nanometer scale cytoskeletal deformation analyses revealed that the strong activation sites of Src by stress colocalized with large deformation sites of microtubules, suggesting that microtubules are essential structures for transmitting stresses to activate cytoplasmic proteins. These results demonstrate that rapid signal transduction via the prestressed cytoskeleton is a unique feature of mechanotransduction.

The sensing and response of living cells and tissues to mechanical forces and physical microenvironments are critical for their functions and survival (1-3). However, the underlying mechanisms remain largely elusive. Various models of mechanotransduction have been proposed (2, 4, 5); the most straightforward model involves force-induced local conformational changes of proteins (6). It is generally believed that similar to soluble ligand-induced signal transduction, mechanotransduction initiates at the local force-membrane interface (e.g., at focal adhesions) by inducing local conformational changes or unfolding of membrane-bound proteins, followed by a cascade of diffusion-based or translocation-based signaling in the cytoplasm. Recent reports demonstrate force-induced dynamic changes in Src activity (7), mechanical extension of the Src family kinase substrate p130Cas (8), and forced unfolding of proteins in living cells (9). However all published reports, including past studies with the reporter type of construct extended here (7), are limited in timescale. Therefore it has not been possible to compare early dynamics of mechanotransduction with that of soluble ligand-induced signal transduction. Here we applied a local stress of physiologic magnitudes and simultaneously imaged changes in Src activity in living cells using a CFP-YFP Src reporter and fluorescent resonance energy transfer (FRET) technology. We show that stress-induced Src activation occurs rapidly in the cytoplasm and depends on the integrity of the microfilaments and microtubules, substrate rigidity, and the cytoskeletal prestress, drastically different from soluble ligand-induced signal transduction.

Results and Discussion

Stress-induced Src activation is rapid. To measure early dynamics of mechanotransduction, we transfected a CFP-YFP cytosolic Src reporter (7) into smooth muscle cells that were plated on collagen-1 coated rigid dishes in the absence of serum and growth factors. Spatio-temporal changes of Src activities were assessed by quantifying changes in FRET ratio of the Src reporter in the cytoplasm. After an Arg-Gly-Asp (RGD) coated magnetic bead (4.5 μm in diameter) was bound to integrin receptors on the cell apical surface for 15 min, a local mechanical stress (step function, 17.5 Pa) was applied to the cell by turning on the magnetic field. This stress induced rapid (<0.3 s), punctuated activation of Src at remote cytoplasmic sites (>20 μm) in individual living cells (Fig. 1*A*, 1*B* and supporting information (SI) Fig. 5). In contrast, Src activation did not occur until 12 s after epidermal growth factor (EGF, ~40 ng/ml on the apical plasma membrane) was released near the cell with a micropipette (<1 μm from micropipette tip to the cell surface) (Fig. 1*C*, 1*D* and SI Fig. 6). Inhibition of Src activity with a specific inhibitor PP1 before or after stimulation prevented or inhibited EGF-induced Src activation (SI Fig. 7). The Src activation by EGF was more uniformly distributed in cytoplasm (SI Fig. 6), quite different from the concentrated Src activation patterns induced by the applied stress. Using a pixel-by-pixel image correlation analysis, the spatial distribution of Src activation by stress was quantified (Fig. 1*E*). There was more Src activation at 10-20 μm away from the bead than at other distances, possibly related to both local cytoskeletal deformation patterns and Src locations in the cytoplasm (see Fig. 3); there was even significant Src activation at distances >50 μm from the localized load within the first 0.3 s stress application (Fig. 1*F* and SI Fig. 8).

Stress-induced Src activation depends on integrin activation, substrate stiffness, prestress, and F-actin integrity. To determine the specificity of the mechanical probe in Src activation, different ligands were coated onto the magnetic bead with the same coating concentration. The bead coated with activating antibody against β1 integrin (clone P4G11) also activated Src, although to a lesser degree than the RGD-coated bead (Fig. 2*A*). Non-activating β1 antibody (clone K20) coated beads did not elicit any Src activation (Fig. 2*A* and SI Fig. 9), possibly due to the fact that these beads do not induce local focal adhesions and thus the applied stress could not penetrate into the deep cytoplasm. This interpretation is supported by the evidence that K20 coated beads do not probe F-actin-dependent cell stiffness (10), suggesting neither focal adhesions nor F-actins were recruited to these beads. Similarly, beads coated with non-adhesion ligand acetylated low density lipoprotein (AcLDL) or nonspecific ligand poly-L-lysine (PLL) did not activate Src (Fig. 2*A* and SI Fig. 9). These results demonstrate that only the stresses applied via activated integrins can induce Src activation.

Recent reports show that substrate rigidity plays a crucial role in regulating cellular functions (1, 2, 11). Individual cells plated on relatively stiff substrates (8 kPa) exhibited stress-induced remote Src activation whereas the cells on soft substrates (0.3 kPa) did not (Fig. 2*B*). Since cells on stiff substrates generate higher prestress than on soft substrates (11), these results suggest that Src activation by applied stress may largely depend on the level of the cytoskeletal prestress in the cell. These data also indicate that the above observed Src activation in cells on collagen-1 coated rigid dishes (see Fig. 1) is not an artifact of the substrate. Interestingly, cells plated on PLL coated rigid dishes failed to exhibit stress-induced remote Src activation using RGD-coated beads (Fig. 2*B*),

consistent with our previously published results that these cells do not exhibit long-distance force propagation due to lack of focal adhesions and tensed actin bundles (12, 13). To further explore the possible role of the actin cytoskeleton and myosin II in stress-induced Src activation, cells were pre-treated with different specific cytoskeletal disrupting agents. As expected, disrupting the actin microfilaments with cytochalasin D (CytoD) or latrunculin A (LatA) prevented Src activation by stress (Fig. 2*C* and SI Fig. 10). Inhibiting myosin II with blebbistatin (Bleb) or cell contractility with dibutyryl adenosine 3'-5' cyclic monophosphate (DBcAMP) all prevented stress-induced Src activation (Fig. 2*C* and SI Fig. 10). Taken together, these results suggest that the myosin II-dependent, tensed, and bundled actin cytoskeleton is necessary for rapid Src activation in the deep cytoplasm.

Stress-induced Src activation colocalizes with microtubule deformation. Published reports show that Src colocalizes with microtubules in adherent cells (14) and that Src localizes at endosomal membranes which are physically associated with microtubules (15, 16). We postulate that microtubules must be deformed in order to induce conformational changes of Src proteins in the deep cytoplasm by stress. To test this hypothesis, we double transfected cells with CFP-YFP Src reporter and mCherry-tubulin. Immediately after recording stress-induced Src activation, stress-induced microtubule deformation images (at the same focal plane) were obtained at high resolution (~5 nm) using the synchronous detection method of periodic loading (12) in the same cell. The strong Src activation sites co-localized with microtubule large displacements/deformation sites (see red arrows in Fig. 3*A*). Out of 19 strong Src activation sites in 4 different cells, 15 were colocalized with microtubule deformation greater than 15 nm (79%); 1 was

colocalized less than 15 nm (5%); 3 sites did not show any apparent colocalization (16%). In contrast, only 12% of strong Src activation sites (3 out of 26) were colocalized with large F-actin deformation sites in 6 different cells (Fig. 3*B*), indicating that F-actin structures were necessary but not sufficient to activate Src. These results suggest that the extent of Src activation depends on the degree of microtubule displacements/deformation and that a threshold of microtubule deformation is necessary for inducing sufficient conformational changes of Src proteins to activate them in the distant cytoplasm (arrowheads in Fig. 3*A* and SI Fig. 11*A*). Consistent with the notion that microtubule deformation is necessary for Src activation in the remote cytoplasm, disrupting microtubules with colchicine prevented stress-induced Src activation (SI Fig. 11*B*). To further explore the potential mechanical and structural basis of Src activation, we quantified microtubule deformation together with endosome deformation/displacements by cotransfecting mCherry-tubulin and GFP-endo into the same cell. We reasoned that for the endosome-membrane bound Src to be activated by direct mechanical deformation, these endosomes must be deformed/displaced locally. Indeed ~80% (10 out of 13) of large endosome displacement (>8 nm) sites were colocalized with large microtubule displacement (>15 nm) sites in 3 different cells (Fig. 3*C*). Taken together, a mechanical/structural pathway for Src activation in the deep cytoplasm appears to emerge: from local loading, focal adhesion and F-actin bundle to transmit stresses to long distances, microtubule deformation, endosome membrane deformation, to Src activation.

Effects of stress and EGF are less than additive. If a threshold of the microtubule-based cytoskeletal deformation exists for Src activation, then Src activation must depend on the magnitude of the applied stress. Indeed Src activation in the cytoplasm is stress-

magnitude dependent: it appears that 1.8 Pa of applied stress was required to activate Src proteins in these smooth muscle cells under these culturing conditions (Fig. 4*A*). Since both stresses and growth factors can independently activate Src proteins, we set out to determine the equivalent global concentration of EGF comparable to the stress applied via focal adhesions at long time periods (up to 15 min). A 1.8-Pa oscillatory stress applied with the magnetic bead via an area of a focal adhesion (~3-5 μm^2) activated Src to the extent equivalent of the effect of 0.4 ng/ml EGF (Fig. 4*B*). With a 1.8-Pa stress at 15 min, the mechanical energy applied to the cell was ~7,000 pN nm (estimated using the applied torque of 515 x 10^3 pN nm times the angular strain of 0.013). With 0.4 ng/ml EGF in the cell medium at 15 min, the chemical energy on the cell surface was ~24,000 pN nm (estimated using the number of surface-bound EGF molecules per cell (17) times thermal energy 1 kT = 6000 x 4 pN nm). It is amazing that the magnitudes of the mechanical energy of 1.8-Pa stress and of the chemical energy of 0.4 ng/ml EGF were within a factor of 4, suggesting that similar magnitudes of energies could cause comparable changes in Src activities.

Since a living spread cell generally has 40-50 focal adhesions (18)**,** if the loading effects were additive, one would predict that this stress applied via 40 focal adhesions simultaneously (e.g., during whole cell stretching) would be equivalent to ~20 ng/ml EGF in activating Src proteins at long times. Interestingly, applying 1.8 Pa stress with 0.4 ng/ml EGF caused an additional 40% increase in Src activation at 15 min, suggesting that the effects of 1.8 Pa stress and 0.4 ng/ml EGF together were less than additive (Fig. 4*B*). As expected, increasing the applied stress magnitude or EGF concentration further elevated Src activation at these long times (Fig. 4*B* and SI Fig. 12).

What is the underlying mechanism for stress-induced rapid Src activation in the remote deep cytoplasm? The prevailing wisdom is that mechanotransduction is initiated at the local force-membrane interface (e.g., at focal adhesions) by inducing local conformational changes or unfolding of membrane-bound proteins, followed by a cascade of diffusion-based or translocation-based signaling in the cytoplasm. The diffusion coefficient D of molecules in the cytoplasm can reach ~60 $\mu m^2/s$ (19). Assuming a distance L of 20 μm from the cell plasma membrane to a site in the deep cytoplasm, then it takes ~1.7 s ($t = L^2/4D = [20\ \mu m]^2/[4x60\ \mu m^2/s]$) to reach the site by diffusion. The translocation speed of proteins via motor proteins on microtubules is ~1-4 μm/s (20). Hence it takes 5-20 s to travel a 20-μm distance. Therefore the rapid (<0.3 s) and long-range (15-60 μm) activation of Src by stress that we have observed cannot be explained by diffusion- or translocation-based mechanisms. In contrast, assuming that the longitudinal elastic wave propagation is applicable to the stress propagation in the cytoplasm along tensed actin bundles (stress fibers), the stress propagation speed is approximately equal to the square root of the ratio of elastic modulus of the stress fiber ($\sim 10^6$ Pa) (21) to the density of the stress fiber ($\sim 10^3$ kg/m^3) and then is ~30 m/s. Thus it would take only ~0.7 μs for the applied stress to travel a 20-μm distance. It is interesting that a stress wave propagation speed of ~30 m/s has been observed in excised lung tissues (22). Taken into account of visco-elasticity of the stress fiber and of the cytoplasm, the traveling time should still be much less than 1 ms to distant places in the cytoplasm in the vicinity of the stress fibers; this theoretical estimation is supported by living cell experimental observation that stresses can propagate to remote cytoplasmic sites (>30 μm) in less than 5 ms (23). We realize that stress fibers rarely exist in vivo, although thin

bundles of myosin filaments and F-actin have been observed in airway smooth muscle tissues (24). Our data on colocalization of microtubule deformation and Src activation (and endosomal membrane deformation) suggest that the microtubule cytoskeleton is an essential structure for transmitting mechanical stresses to activate cytoplasmic proteins. How do we explain the current experimental results that Src is only slightly activated after the first 100 ms stress application (Fig. 1*B*)? It is reported that the time constant for Src activation in vitro is ~200 ms; the rate limiting factor is not phosphoryl transfer but appears to be associated with the conformational change of the enzyme (25). Therefore the time of ~300 ms for the stress-induced Src activation that we have observed in living cells is likely due to the time delays in conformational changes of Src, in physical association of Src with its substrate reporter, and in conformational changes of the reporter. This interpretation does not rule out the possibility that other molecules (e.g., stretch-sensitive ion channels in cell membrane) are activated by stress before Src activation, but these potentially activated molecules (including calcium) cannot travel fast enough to the remote cytoplasmic sites to activate Src within 300 ms.

At the present time, the exact mechanical basis for the rapid activation of Src at remote sites of the cytoplasm is not clear. In fact, based on mechanical principles of homogeneous continuum materials (*St*. Venant's principle), one would predict that a local mechanical load of physiologic magnitudes should only cause a local deformation. Therefore the prevailing wisdom is that a local stress should cause *only* local direct mechanotransduction based on local conformational changes or unfolding of proteins at the force-cell interface (e.g., a focal adhesion). The magnitudes of the applied forces are important in living cells since it has been observed that high amplitude forces applied to

fibroblasts for hours (>4 hrs) can cause apoptosis (26). During the last few years, the long distance stress propagation in the cytoplasm and into the nucleus of living cells has been observed (12, 13, 27) and a theoretical composite model of the cytoskeleton has been proposed to interpret the behavior of long distance force propagation (28). However, still no experimental data of rapid direct mechanotranduction were available. Here we show for the first time that stress-induced signal transduction is at least 40 times faster than growth factor-induced signal transduction. Importantly, almost simultaneous activation of enzymes at remote discrete sites in the deep cytoplasm as well as at local sites by localized mechanical stresses with physiologic magnitudes challenges the current thinking about mechanical-chemical signal transduction pathways. In sharp contrast, membrane-bound molecules in soluble growth factor-induced signal transduction are activated first, followed by a sequential activation of cytosplasmic molecules in space away from the plasma membrane via diffusion or translocation based mechanisms. The kinetics of stress-induced Src activation appears to be different from that of EGF-induced Src activation. We do not know the underlying mechanism for this difference, but a similar kinetics has been observed in flow shear-induced Ras activation in endothelial cells (29), suggesting that it might be a general feature of stress-induced protein activation. Our working model for rapid mechanotranduction is that a focal adhesion and a tensed cytoskeleton are necessary for long distance force propagation in the cytoplasm to cause microtubule displacements/deformations, which, in turn, are necessary for causing conformational changes of proteins for signal transduction. Our findings significantly extend previous work (7, 9) and provide experimental evidence for the unique feature of local stress-induced signal transduction.

Other features of mechanotransduction have been demonstrated in recent years: myosin-dependent substrate rigidity feedback (11, 30), myosin-dependent periodic lamellipodial contractions (31), selective recruitment of adaptor proteins by shear flow stress (32), stress-induced alterations of dissociation constant of focal adhesion zyxin proteins (33), and force-induced structural adaptation at focal adhesions (34) and mechanical adaptation at focal adhesions (35) or in the whole cell (36). It remains to be seen how the rapid activation of Src (and possibly other signaling molecules such as Rac or Rho (37)) by stress might be involved in myosin-dependent mechanochemical feedback and cellular remodeling and adaptation. Eventually one would like to know how a living cell integrates local and distant effects of mechanical stimulation with soluble factor stimulation into a cohesive biological response such as gene expression.

Materials and Methods

Cell Culture and Transfections. Human airway smooth muscle (HASM) cells were isolated from tracheal muscle obtained from lung transplant donors and cultured as described previously (12). Cell culture reagents were obtained from Invitrogen unless otherwise noted. HASM cells were serum deprived and supplemented with 5.7 μg/ml insulin (Sigma) and 5 μg/ml human transferrin (Sigma) for 36-48 h before the experiments. A genetically encoded, cytosolic CFP-YFP Src reporter was developed and its specificity was tested as described previously (7). A variant, more sensitive form of this probe was developed by replacing the FRET acceptor with YPet and specificity-tested. Both biosensors yielded the same specificity. mCherry-tubulin and mCherry-actin probes were gifts from Dr. R. Tsien's lab. HASM cells (passages 3-8), plated on type I collagen-coated (20 μg/ml) rigid dishes, poly-L-lysine-coated (20 μg/ml) rigid dishes, or type I collagen- coated (100 μg/ml) polyacrylamide gels, were transfected with CFP-YFP cytosolic Src reporter and/or mCherry-tubulin, mCherry-actin and CFP-YFP Src reporter, or mCherry-tubulin and pAcGFP1-endo that targets endosome membrane (Clontech), using the lipofectamine method following protocols provided by the manufacturer (Invitrogen).

Inhibitors and Antibodies. Latrunculin A (LatA), cytochalasin D (CytoD), dibutyryl adenosine 3'-5' cyclic monophosphate (DBcAMP) and colchicine were from Sigma. Blebbistatin (Bleb) was from Toronto Research Chemicals. A mouse monoclonal anti-integrin β_1 activating antibody (clone P4G11) was from Chemicon. A mouse monoclonal

anti-integrin β_1 non-activating antibody (clone K20) was from Santa Cruz Biotechnology. Src-selective tyrosine kinase inhibitor, 4-Amino-5-(4-methylphenyl)-7-(t-butyl) parasol (3,4-d)-pyrimidine (PP1) was from Biomol.

Magnetic Bead Coating. Ferromagnetic beads (Fe_3O_4, 4.5 μm in diameter) were coated with Arg-Gly-Asp (RGD; Integra), integrin β_1 activating antibody (P4G11), integrin β_1 non-activating antibody (K20), acetylated low-density lipoprotein (AcLDL), or poly-L-lysine (PLL), all at 50 μg/ml per mg bead as described (38). The binding specificity was determined (38). The magnetic moment constant of the bead was calibrated in a viscous standard and determined to be 3.5 dynes/cm^2 per gauss (39). A single bead bound to the apex of the cell body (but not the portion of filopodia or lamellipodia to avoid rigid substrate effects) was chosen for experiment. The bead-cell contact area was ~5 μm^2 and did not change much during the course of the experiments.

Polyacrylamide Gels. The polyacrylamide gels were prepared as described (30). The elastic Young's modulus of the polyacrylamide gels used in this study was 0.3 kPa (0.04% bisacrylamide and 3% acrylamide) and 8 kPa (0.3% bisacrylamide and 5% acrylamide) (11).

EGF Stimulation. A micropipette (Eppendorf; 25 μm inside diameter) backfilled with 50 ng/ml EGF was controlled using a micromanipulator (InjectMan NI2; Eppendorf). EGF was released 0.5-1 μm above the cell apical surface (SI Fig. 6) at a flow rate of 2x10^4 μm^3/ms using a piston pump (CellTram vario; Eppendorf). During imaging, the cells were maintained in Hank's balanced salt solution with 20 mM HEPES and 2 g/l D-glucose (7).

Magnetic Twisting Cytometry and Microscopy. The technique of magnetic twisting cytometry was described previously (10, 38). The magnetic twisting field was varied at 0, 2, 5, 10, 25, 50, or 70 gauss, either a step function or a sinusoidal oscillatory wave at 0.3 Hz. The apparent applied stress is defined as the ratio of the applied torque to six times the bead volume and equals the bead constant times the applied twisting field. Thus the applied stress was 0, 0.7, 1.8, 3.5, 8.8, 17.5, 24.5 Pa corresponding to the above applied magnetic fields respectively.

A Leica inverted microscope was integrated with a magnetic twisting device and a Dual-View system (Optical Insights) to simultaneously acquire both CFP and YFP emission images in response to stress. For emission ratio imaging, the Dual-View Micro-Imager (Optical Insights, Tucson, AZ) was used. CFP/YFP Dual EX/EM (FRET) (OI-04-SEX2) has the following filter sets: CFP: excitation, S430/25, emission S470/30; YFP: excitation, S500/20, emission S535/30. The emission filter set uses a 515 nm dichroic mirror to split the two emission images. Cells were illuminated with a 100W Hg lamp. For FRET imaging, each CFP (1344 pixels by 512 pixels) and each YFP image (1344 pixels by 512 pixels) were simultaneously captured on the same screen using a CCD camera (Hamamatsu C4742-95-12ERG) and a 40X 0.55NA air or a 63X 1.32NA oil-immersion objective. Exposure time was 89.3 ms for the first data point collecting at 100 ms after stress and was 273 ms for subsequent images.

To acquire mCherry-tubulin containing microtubule displacement images, we applied oscillatory mechanical torques to the magnetic bead attached to the cell and the stress-induced synchronized movements of the microtubules were quantified using the synchronous detection method (12). This sensitive method can detect displacements or

deformation of cytoskeletal structures to the resolution of 4-5 nm (27). Microtubule images were obtained every 0.32 s using a 63X 1.32NA oil-immersion objective with 290 ms exposure time using a N2.1 filter set (BP 515-560, Dichromatic mirror 580, and LP 590).

Image Analysis. We developed a customized Matlab (Mathworks) program to obtain CFP/YFP emission ratio images. CFP and YFP images at each time point were first background-subtracted and the YFP image was thresholded to generate a binary mask so that the pixel value inside the cell was set to 1 and the pixel value outside the cell was set to 0. After multiplication of the original CFP image by the mask image, this updated CFP image and the YFP image were aligned pixel-by-pixel by maximizing the normalized cross-correlation coefficient of the CFP and YFP images (7). Aligned CFP/YFP emission ratios were normalized to the lower emission ratio and displayed as a linear pseudocolor. To increase the sensitivity of the mean emission ratios, nucleus regions were excluded because the pixel values within a nucleus region did not change before and after stimulation. Two-tailed Student t-test was used for all statistical analyses.

ACKNOWLEDGMENTS. We thank Dr. R. Tsien for the gift of mCherry-tubulin and mCherry-actin probes, Dr. R. Panettieri for providing the cells, Dr. J. Jorgensen for sharing facilities, B. Kim, Y. Kim, and N. Gidwani for assistance. This work was supported by NIH grant GM072744 (N.W.), University of Illinois (N.W.), and Wallace H. Coulter Foundation and Beckman Laser Institute Inc. Foundation (Y.W.).

References

1. Discher DE, Janmey P, Wang YL (2005) Tissue cells feel and respond to the stiffness of their substrate. *Science* 310:1139-1143.
2. Giannone G, Sheetz MP (2006) Substrate rigidity and force define form through tyrosine phosphatase and kinase pathways. *Trends Cell Biol* 16:213-223.
3. Janmey PA, McCulloch CA (2007) Cell mechanics: integrating cell responses to mechanical stimuli. *Annu Rev Biomed Eng* 9:1-34.
4. Orr AW, Helmke BP, Blackman BR, Schwartz MA (2006) Mechanisms of mechanotransduction. *Dev Cell* 10:11-20.
5. Ingber DE (2006) Cellular mechanotransduction: putting all the pieces together again. *FASEB J* 20:811-827.
6. Vogel V, Sheetz M (2006) Local force and geometry sensing regulate cell functions. *Nat Rev Mol Cell Biol* 7:265-275.
7. Wang Y *et al.* (2005) Visualizing the mechanical activation of Src. *Nature* 434:1040-1045.
8. Sawada Y *et al.* (2006) Force sensing by mechanical extension of the Src family kinase substrate p130Cas. *Cell* 127:1015-1026.
9. Johnson CP *et al.* (2007) Forced unfolding of proteins within cells. *Science* 317:663-666.
10. Puig-de-Morales M *et al.* (2004) Cytoskeletal mechanics in adherent human airway smooth muscle cells: probe specificity and scaling of protein-protein dynamics. *Am J Physiol Cell Physiol* 287:C643-C654.

11. Engler AJ, Sen S, Sweeney HL, Discher DE (2006) Matrix elasticity directs stem cell lineage specification. *Cell* 126:677-689.

12. Hu S *et al.* (2003) Intracellular stress tomography reveals stress focusing and structural anisotropy in cytoskeleton of living cells. *Am J Physiol Cell Physiol* 285:C1082-C1090.

13. Hu S, Chen J, Butler JP, Wang N (2005) Prestress mediates force propagation into the nucleus. *Biochem Biophys Res Commun* 329:423-428.

14. Abu-Amer Y *et al.* (1997) Substrate recognition by osteoclast precursors induces C-src/microtubule association. *J Cell Biol* 137:247-258.

15. Kaplan KB, Swedlow JR, Varmus HE, Morgan DO (1992) Association of p60c-src with endosomal membranes in mammalian fibroblasts. *J Cell Biol* 118:321-333.

16. Loubéry S *et al.* (2008) Different microtubule motors move early and late endocytic compartments. *Traffic* [Jan 10; Epub ahead of print].

17. Wiley HS, Cunningham DD (1981) A steady state model for analyzing the cellular binding, internalization and degradation of polypeptide ligands. *Cell* 25:433-440.

18. Boguslavsky S *et al.* (2007) P120 catenin regulates lamellipodial dynamics and cell adhesion in cooperation with cortactin. *Proc Natl Acad Sci USA* 104:10882-10887.

19. Costa M *et al.* (2006) Dynamic regulation of ERK2 nuclear translocation and mobility in living cells. *J Cell Sci* 119:4952-4963.

20. Kural C *et al.* (2005) Kinesin and dynein move a peroxisome in vivo: a tug-of-war or coordinated movement? *Science* 308:1469-1472.

21. Deguchi S, Ohashi T, Sato M (2006) Tensile properties of single stress fibers isolated from cultured vascular smooth muscle cells. *J Biomech* 39:2603-2610.

22. Yen RT, Fung YC, Ho HH, Butterman G (1986) Speed of stress wave propagation in lung. *J Appl Physiol* 61:701-705.

23. Hu S, Wang N (2006) Control of stress propagation in the cytoplasm by prestress and loading frequency. *Mol Cell Biomech* 3:49-60.

24. Kuo K-H, Seow CY (2004) Contractile filament architecture and force transmission in swine airway smooth muscle. *J Cell Sci* 117:1503-1511.

25. Lieser SA *et al.* (2005) Phosphoryl transfer step in the C-terminal Src kinase controls Src recognition. *J Biol Chem* 280:7769-7776.

26. Kainulainen T et al. (2002) Cell death and mechanoprotection by filamin A connective tissues after challenge by applied tensile forces. *J Biol Chem* 277: 21998-22009.

27. Hu S *et al.* (2004) Mechanical anisotropy of adherent cells probed by a three-dimensional magnetic twisting device. *Am J Physiol Cell Physiol* 287:C1184-C1191.

28. Wang N, Suo Z (2005) Long-distance propagation of forces in a cell. *Biochem Biophys Res Commun* 328:1133-1138.

29. Gudi S *et al*. (2003) Rapid activation of Ras by fluid flow is mediated by $G\alpha_q$ and $G\beta\gamma$ subunits of heterotrimeric G proteins in human endothelial cells. *Arterioscler Thromb Vasc Biol* 23:994-1000.

30. Pelham RJ Jr, Wang YL (1997) Cell locomotion and focal adhesions are regulated by substrate flexibility. *Proc Natl Acad Sci USA* 94:13661-13665.

31. Giannone G *et al.* (2004) Periodic lamellipodial contractions correlate with rearward actin waves. *Cell* 116:431-443.

32. Wang Y *et al.* (2007) Selective adapter recruitment and differential signaling networks by VEGF vs. shear stress. *Proc Natl Acad Sci USA* 104:8875-8879.

33. Lele TP *et al.* (2006) Mechanical forces alter zyxin unbinding kinetics within focal adhesions of living cells. *J Cell Physiol* 207:187-194.

34. Riveline D *et al.* (2001) Focal contacts as mechanosensors: externally applied local mechanical force induces growth of focal contacts by an mDia1-dependent and ROCK-independent mechanism. *J Cell Biol* 153:1175-1186.

35. Matthews BD, Overby DR, Mannix R, Ingber DE (2006) Cellular adaptation to mechanical stress: role of integrins, Rho, cytoskeletal tension and mechanosensitive ion channels. *J Cell Sci* 119:508-518.

36. Trepat X *et al.* (2007) Universal physical responses to stretch in the living cell. *Nature* 447:592-595.

37. Pertz O, Hodgson L, Klemke RL, Hahn KM (2006) Spatiotemporal dynamics of RhoA activity in migrating cells. *Nature* 440:1069-1072.

38. Wang N, Butler JP, Ingber DE (1993) Mechanotransduction across the cell surface and through the cytoskeleton. *Science* 260:1124-1127.

39. Brune D, Kim S (1993) Predicting protein diffusion coefficients. *Proc Natl Acad Sci USA* 90:3835-3839.

Figure Legends

Fig. 1. Rapid Src activation in response to localized mechanical stress. (*A*) A 4.5-μm RGD-coated ferromagnetic bead was attached to the apical surface of the cell (left top image, black dot is the bead) for 15 min to allow integrin clustering and formation of focal adhesions around the bead (37). Bead binding alone induced little Src activation (SI Fig. 13). The bead was magnetized horizontally and subjected to a vertical magnetic field (step function) which applies a mechanical stress σ (specific torque=17.5 Pa) to the cell. A genetically encoded, CFP-YFP cytosolic Src reporter was transfected into the smooth muscle cells following published procedures (7). The cytosolic Src reporter was uniformly distributed in the cytoplasm (left bottom image, YFP). The stress application induced rapid changes (<0.3 s) in FRET of the Src reporter at discrete, distant sites in the cytoplasm (see inserts) (focal plane is ~1 μm above cell base), indicating rapid Src activation (SI Fig. 5). Images are scaled and regions of large FRET changes (strong Src activity) are shown in red. Black arrow indicates bead movement direction. Scale bar = 10 μm. (*B*) Time course of normalized CFP/YFP emission ratio, an index of Src activation in response to mechanical or soluble growth factor EGF stimulation. n = 12 cells for $+\sigma$, n = 8 cells for +EGF. Error bars represent SEM. (*C*) Time course of normalized CFP/YFP emission ratio in response to EGF in a representative cell (see SI Fig. 6 for full time course). EGF was locally released on top of the cell apical surface (<1 μm above) using a micropipette (25 μm in diameter; top right of the insert; scale bar = 20 μm) which was controlled by a micromanipulator and *CellTram Vario*. EGF (50 ng/ml) was released at a flow rate of 2 x 10^4 μm^3/ms continuously for 5 min. Since the diffusion

coefficient of a protein in water is ~100 $\mu m^2/s$ (39), it takes ~10 ms for EGF to reach the cell apical surface and local EGF concentration at the cell apical surface is ~40 ng/ml. (*D*) Time course of average Src activation from 8 different cells after EGF treatment as in (*C*). Error bars represent SEM. (*E*) Src activation at different cytoplasmic sites. At every 1-μm away from the bead, emission ratio image after mechanical stimulation was compared pixel-by-pixel with that before mechanical stimulation. (*F*) The number of activated pixels (percentage of total activated pixels) at a given time versus distance from the bead after 0.3 s and 2.7 s of mechanical stimulation (see SI Fig. 8 with 90% threshold). Maximum number of Src activation was observed at ~15 μm away from the bead. Note that the spatial distribution of Src activation but not the intensity of Src activation is summarized here. n = 8 cells. Error bars represent SEM.

Fig. 2. Src activation depends on stress probe specificity, substrate rigidity, intact F-actin, and prestress. (*A*) Probe specificity on Src activation. Mechanical stimulation via the magnetic bead coated with RGD or anti-β_1 activating antibody (P4G11), induced Src activation in the cytoplasm, but not anti-β_1 non-activating antibody (K20), AcLDL (binds scavenger receptors), or PLL (strong nonspecific surface binding) (SI Fig. 9). RGD, n = 12 cells; P4G11, n = 4 cells; K20, n = 3 cells; AcLDL, n = 4 cells; PLL, n = 3 cells. Error bars represent SEM. (*B*) Mechanical stimulation of cells plated on soft (0.3 kPa, n = 10 cells) polyacrylamide gel substrate did not induce Src activation, whereas the cell on relatively hard (8 kPa, n = 4 cells) substrate induced strong Src activation (red arrows). Cells on PLL substrate (n = 8 cells) that do not form basal focal adhesions and stress fibers (12) did not activate Src in response to mechanical stress. White arrows indicate

magnetic bead movement direction (stress = 17.5 Pa). Scale bars = 10 μm. (*C*) Preincubating cells with CytoD (1 μg/ml for 15 min; n = 5 cells), LatA (1 μM for 15 min; n = 4 cells) to disrupt actin microfilaments, Bleb (50 μM for 20 min; n = 5 cells) to inhibit myosin II, or DBcAMP (1 mM for 15 min; n = 4 cells) to relax the cell, prevented stress-induced Src activation (SI Fig. 10).

Fig. 3. Rapid, long-range strong Src activation sites in the cytoplasm co-localize with sites of large microtubule displacements. (*A*) The cell was co-transfected with CFP-YFP Src reporter and mCherry-tubulin. A step function stress (17.5 Pa) was first applied for 3 s via an RGD-coated bead and FRET changes were recorded. Then microtubule deformation map was acquired when an oscillatory stress was applied for ~30 s (0.3 Hz; peak stress = 24.5 Pa, equivalent to a constant stress of 17.5 Pa) (12). In this representative cell, strong Src activation sites coincide with large deformation sites (>15 nm) of microtubules in the same cell at the same focal plane (~1 μm above cell base). The overlay image is the YFP Src reporter image superimposed with the bead. Pink circle indicates bead center position; white arrows represent microtubule deformation direction. Red arrows point to strong Src activation sites. In colocalization analysis panel, red represents strong Src activation and black lines represent large microtubule displacements. 3 other different cells showed similar results. Of strong Src activation sites, ~80% (15 out of 19) were colocalized with sites of microtubule deformation greater than 15 nm. Scale bar = 10 μm. (*B*) Src activation sites do not colocalize with F-actin deformation sites. The cell was co-transfected with CFP-YFP Src reporter and mCherry-actin. A step function stress (17.5 Pa) was first applied for 3 s via an RGD-coated bead

and FRET changes were recorded. Then actin deformation map was acquired when an oscillatory stress was applied the same way as in (*A*). In contrast to (*A*), strong Src activation sites do not coincide with large deformation sites (>15 nm) of actin in the same cell at the same focal plane (~1 μm above cell base). Pink circle indicates bead center position; white arrows represent actin deformation direction. In colocalization analysis panel, red represents strong Src activation and black lines represent large actin displacements greater than 15 nm. 5 other different cells showed similar results. Of strong Src activation sites, only ~12% (3 out of 26) were colocalized with sites of actin deformation greater than 15 nm. Scale bar = 10 μm. (*C*) Large microtubule deformation sites colocalize with endosomal membrane deformation in the same cell at the same focal plane (~1 μm above cell base). The insert is the bright field image of the cell. The cell was co-transfected with mCherry-tubulin and pAcGFP1-endo (left panel). The displacement maps of microtubule and endosome were acquired when an oscillatory stress was applied separately (30 sec each) (peak stress = 24.5 Pa, frequency = 0.3 Hz). In colocalization panel, red represents microtubule displacements greater than 15 nm, green represents endosome displacements greater than 8 nm, and overlapped black shows colocalization sites of microtubule and endosome. Out of 13 large endosome displacement sites in 3 different cells, 10 were colocalized (~80%) with large microtubule deformation sites. Scale bar unit of the displacement map is nm. Scale bar = 10 μm.

Fig. 4. Src activity in response to mechanical and/or EGF stimulation at long times. (*A*) Src activation is stress-magnitude dependent. n = 12 cells for stress of 17.5 Pa; 4 for 8.8

Pa; 4 for 3.5 Pa; 4 for 1.8 Pa; 3 for 0.7 Pa. It appears that Src is activated when the applied stress is greater than 1.8 Pa. Error bars represent SEM. (*B*) Stress magnitude equivalent of EGF concentration. A 1.8-Pa oscillatory stress activated Src to the same extent as 0.4 ng/ml EGF (final global concentration). Stress together with EGF further increased Src activation by ~40% at 15 min, suggesting less than additive effects. P values are 0.027, 0.036, and 0.005 between 1.8 Pa + 0.4 ng/ml and 0.4 ng/ml for 5, 10, 15 min; p values are 0.024, 0.021, and 0.047 between 1.8 Pa + 0.4 ng/ml and 1.8 Pa for 5, 10 and 15 min. n = 4 cells for 0.5 ng/ml; 3 for 0.4 ng/ml; 3 for 0.005 ng/ml; 3 for 24.5 Pa; 7 for 1.8 Pa + 0.4 ng/ml; 6 for 1.8 Pa. Error bars represent SEM.

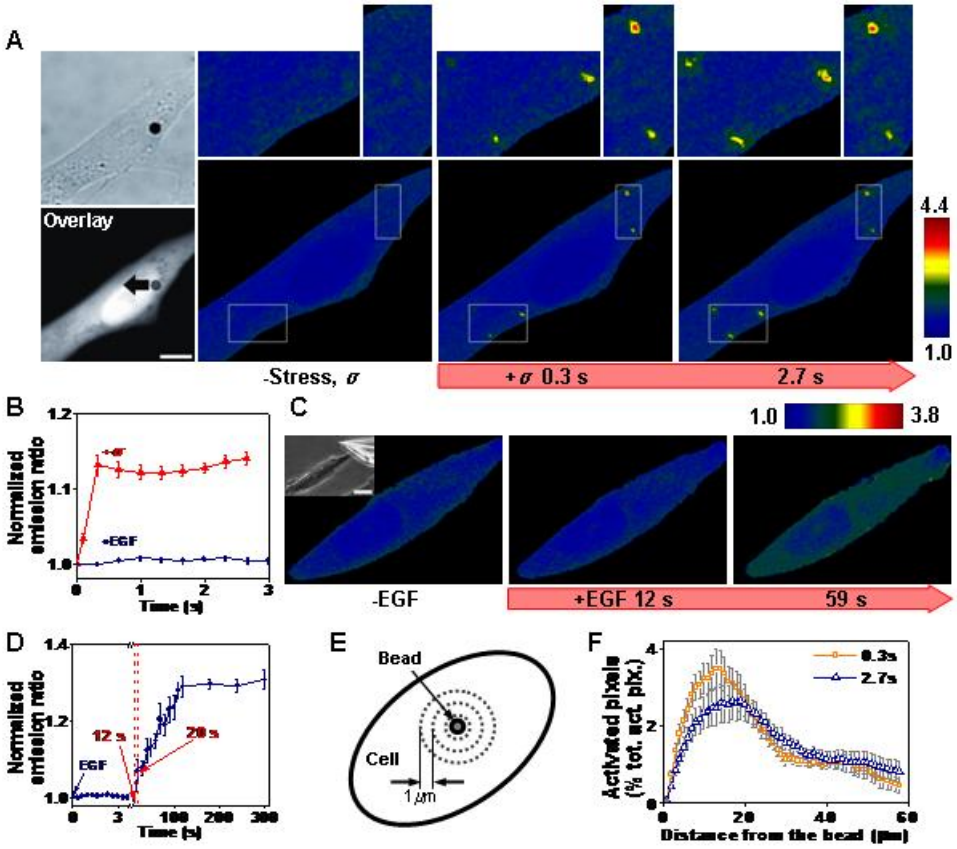
A
Overlay
4.4
1.0
-Stress, σ
+σ 0.3 s
2.7 s
B
Normalized emission ratio
+σ
+EGF
Time (s)
C
1.0
3.8
-EGF
+EGF 12 s
59 s
D
Normalized emission ratio
12 s
20 s
EGF
Time (s)
E
Bead
Cell
1 μm
F
Activated pixels (% tot. act. pix.)
0.3s
2.7s
Distance from the bead (μm)

Fig. 1

26

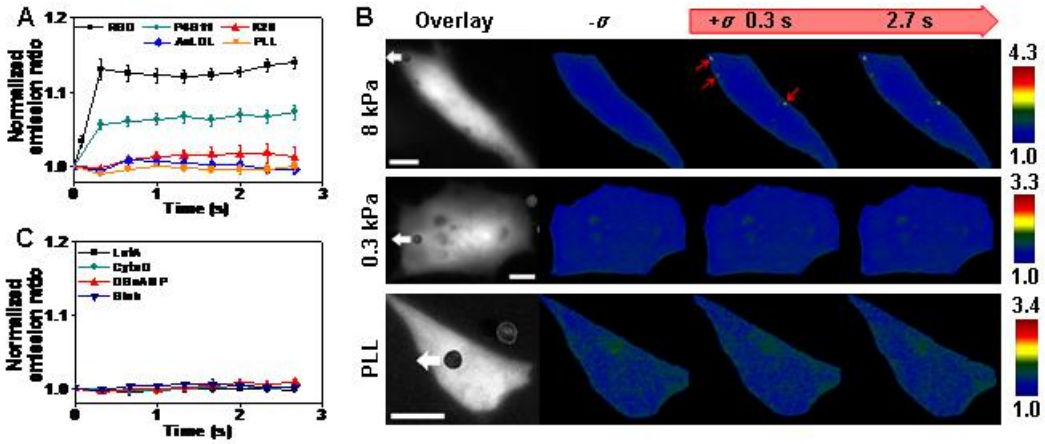
A
Normalized emission ratio
Time (s)
C
Normalized emission ratio
Time (s)
B
Overlay
-σ
+σ 0.3 s
2.7 s
8 kPa
0.3 kPa
PLL
4.3
1.0
3.3
1.0
3.4
1.0

Fig. 2

27

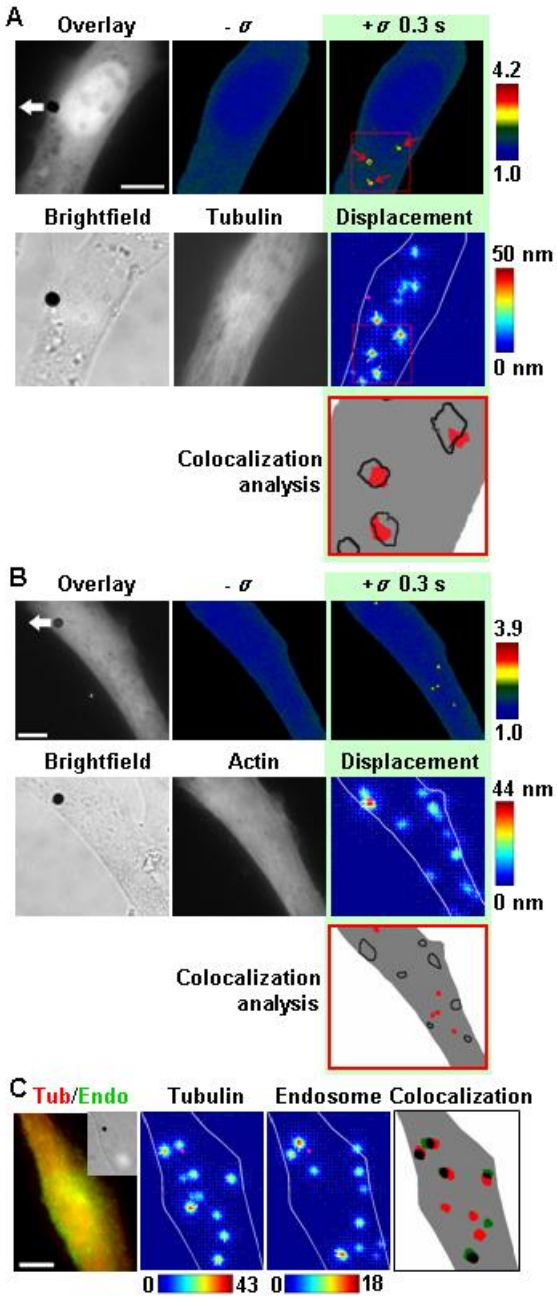
A
Overlay
- σ
+σ 0.3 s
4.2
1.0
Brightfield
Tubulin
Displacement
50 nm
0 nm
Colocalization analysis
B
Overlay
- σ
+σ 0.3 s
3.9
1.0
Brightfield
Actin
Displacement
44 nm
0 nm
Colocalization analysis
C
Tub/Endo
Tubulin
Endosome
Colocalization
0
43
0
18

Fig. 3

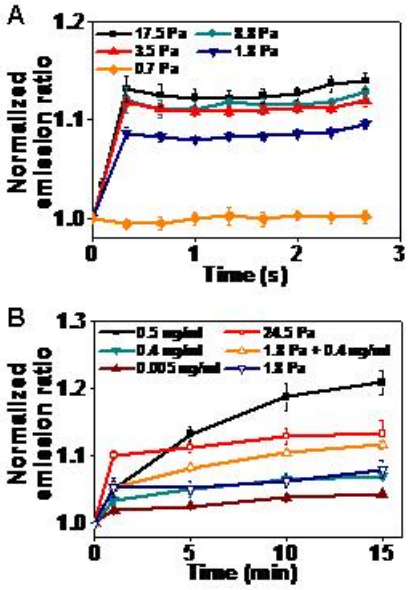
A
Normalized emission ratio
17.5 Pa
8.8 Pa
3.5 Pa
1.8 Pa
0.7 Pa
Time (s)
B
Normalized emission ratio
0.5 mg/ml
24.5 Pa
0.4 mg/ml
1.8 Pa + 0.4 mg/ml
0.005 mg/ml
1.8 Pa
Time (min)

Fig. 4

29